Quantum vortices and thermally induced luminescence of nitrogen nanoclusters immersed in liquid helium

A. Meraki,[1] P. T. McColgan,[1] P. M. Rentzepis,[2] R. Z. Li,[2] D. M. Lee,[1] and V. V. Khmelenko[1,*]

[1]*Department of Physics and Astronomy and Institute for Quantum Science and Engineering, Texas A&M University, College Station, Texas 77843, USA*

[2]*Department of Electrical and Computer Engineering, Texas A&M University, College Station, Texas 77843, USA*

(Received 12 July 2016; revised manuscript received 9 February 2017; published 1 March 2017; corrected 9 November 2020)

We performed investigations of ensembles of molecular nitrogen nanoclusters, containing stabilized nitrogen atoms, immersed in liquid helium by electron spin resonance and optical spectroscopy. We observed thermoluminescence of nitrogen atoms and molecules via increasing temperature from 1.25 to 4.4 K. Two thermoluminescence maxima were observed, one in superfluid helium (HeII) at $T \sim 1.9$ K and another in normal helium (HeI) at $T \sim 3.2$ K. We explain appearance of luminescence in HeII by chemical reactions of nitrogen atoms on surfaces of nanoclusters which might be initiated by quantum vortices. Thermoluminescence in HeI occurs due to the process of nanocluster association resulting in thermal explosions of a small fraction of nanoclusters. This research might open new possibilities for studying a broad range of chemical reactions initiated by quantum vortices in HeII.

DOI: 10.1103/PhysRevB.95.104502

I. INTRODUCTION

Investigations of quantum turbulence in superfluid helium (HeII) have recently attracted great attention [1–3]. Considerable progress in this area of research has been achieved due to new experimental methods [4–8]. The visualization of vortex cores has led to the observation of the reconnection of vortices and direct observation of Kelvin waves excited by quantized vortex reconnections [9,10]. The dissipation of quantum turbulence was studied at the zero temperature limit [11,12]. The technique of nanowire formation by ablating metallic nanoparticles from a target in HeII was realized on the basis of coalescence of the nanoparticles on the vortices [13,14]. All of these investigations were performed in bulk superfluid helium. Investigations of quantum turbulence in restricted geometries are challenging. An example of this type of study is the investigation of quantum vortices inside free superfluid droplets with sizes ranging from 100 to 1000 μm [15,16]. Recently, the dynamics of vortices and turbulent behavior have been investigated in atomic gas Bose-Einstein condensates [17].

In the past, many theoretical and experimental studies of the behavior of liquid helium in porous restricted geometries were performed [18,19]. Liquid helium has long provided a testing ground for theories of phase transitions. Finite size effects might shift or smear out phase transitions. The multiple-connected substrate geometry may change the effective dimensionality, or the disorder induced by the porous material may change the nature of the transition [20,21].

Here we present a unique means for investigating the influence of the quantum properties of liquid helium on the behavior of porous ensembles of nitrogen nanoclusters containing stabilized nitrogen atoms. Simultaneous measurements of the characteristics of stabilized nitrogen atoms by the electron spin resonance method and thermoluminescence of the nanoclusters by optical spectroscopy were performed. We observed thermoluminescence of nitrogen atoms and molecules in molecular nanoclusters immersed in liquid helium while increasing the temperature from 1.25 to 4.4 K. Two thermoluminescence maxima were observed, one in superfluid helium at $T \sim 1.9$ K and another at $T \sim 3.2$ K. The thermoluminescence in HeII was found to be a result of chemical reactions of nitrogen atoms residing on surfaces of nanoclusters, which might be initiated by quantum vortices.

Impurity-helium condensates are composed of aggregations of nanoclusters. The nanoclusters form an extremely porous gel-like material into which liquid helium can easily penetrate [22,23]. The characteristic size of each nanocluster is of the order of 5 nm and the density of the impurities inside liquid helium is of the order of 10^{20} cm^{-3} as determined from x-ray experiments [22]. Ultrasound studies gave estimates for the pore sizes, which varied from 8 to 860 nm, and also provided evidence for the presence of large size voids in the samples [24]. In our experiments, nitrogen atoms were captured mainly on the surface of the molecular nitrogen nanoclusters [25]. The average concentration of nitrogen atoms in nitrogen-helium condensates may be as high as 10^{19} cm^{-3} [26].

II. EXPERIMENTAL APPARATUS

In this work, optical and electron spin resonance spectroscopies were used to investigate ensembles of nanoclusters immersed in liquid helium during annealing from 1.5 to 4.4 K. Aggregates of molecular nitrogen nanoclusters immersed in HeII were produced by injection of a gaseous helium jet containing a small admixture of nitrogen molecules ($\sim$0.125%–1%) passing through a radio-frequency discharge into superfluid helium [27]. This method has been used for the successful creation of ensembles of nanoclusters in HeII from a variety of impurities [28,29]. In the experiment, we used research grade helium gas from Linde Electronics&Specialty Gases with 99.9999% purity. The oxygen content in the gas mixture ($\sim$1 ppm) results from contamination of the

*khmel@physics.tamu.edu

helium gas. The flux of 5×10^{19} atoms per second of the nitrogen-helium mixture is measured by a Brooks Instrument 5850E flow controller. During sample collection a temperature of 1.5 K of the liquid helium in the sample tube was maintained by pumping the helium bath and was measured by germanium thermometers. The level of liquid helium in the sample tube was measured by a superconducting wire sensor connected to an LM500 level meter. A beaker for collecting samples was placed below an orifice at the capillary outlet at a distance of 2.5 cm. The sample accumulation lasted ∼10 min. The helium level in the sample beaker was maintained by a fountain pump during the sample preparation process.

After finishing the sample collection into the lower cylindrical section, the beaker was lowered into the electron spin resonance (ESR) cavity. The cavity operated in the TE_{011} mode and was situated at the bottom of the cryostat in the center of an electromagnet. Quartz windows and holes in the cavity allowed optical access to the sample. The lower part of the cryostat with the experimental cell is shown in Fig. 1(a). For recording of the ESR spectra of stabilized atoms, we used a Bruker EPR EMX console. The ESR method provides the spectroscopic signature for N atoms stabilized in solid matrices. Linewidth, hyperfine splitting and g factor can be obtained from the shape and position of the ESR lines. From these data, the average and local concentration of N atoms were determined in our work. To obtain the average concentration of N(^{4}S), we permanently placed a ruby crystal at the bottom of the microwave cavity [see 8 in Fig. 1(a)], and calibration of the signal from the ruby crystal was made by reference to a sample of diphenyl-picrylhydrazil (DPPH), with a known number of spins $\sim 2.4 \times 10^{17}$. We thus used the ruby crystal as a secondary standard.

In the experiments, the luminescence from the samples was focused by a lens onto the end of an optical fiber [see 13 in Fig. 1(a)]. The fiber transfers light to the entrance of an Andor Shamrock SR500 spectrograph. The Andor spectrograph with a Newton EMCCD camera was used to obtain high resolution (up to 0.05 nm) optical spectra in the wavelength range between 200 and 1100 nm. All optical spectra presented in this paper are corrected for the quantum efficiency of the registration system [30].

We performed measurements of the temperature dependence of the temperature gradient developing in liquid helium in the vertical direction during the process of warming our samples. Two thermometers were separated by a distance 20.5 cm in the vertical direction [see 3 and 12 in Fig. 1(a)]. These measurements were repeated three times and the averaged curve for temperature gradient is shown in Fig. 1(b). The largest gradient ($\sim 6 \times 10^{-4}$ K cm^{-1}) was observed at the lowest temperatures and the smallest one ($\sim 1 \times 10^{-4}$ K cm^{-1}) at temperatures close to T_λ. This result is in qualitative agreement with the expected behavior for the temperature gradient in the case of a small heat flux [31]. We estimated the heat flux from the measurements of the volume of evaporated helium during the warming of liquid helium from 1.3 to 2.165 K and cooling back. The volume of evaporated helium was determined from the measurement of the level of liquid helium at the temperature before heating up and after cooling back down. The estimated average heat flux during the warming up process was of order 25–30 mW cm^{-2}.

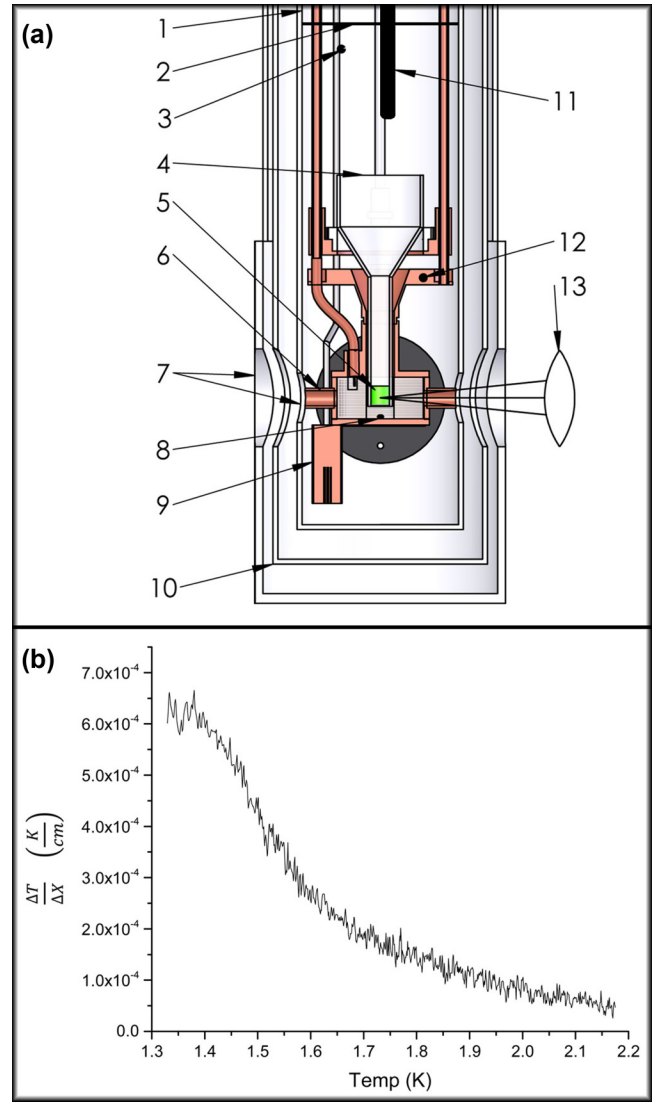

FIG. 1. (a) Schematic of the setup for electron spin resonance and optical spectroscopy studies of the ensembles of nanoclusters immersed in liquid helium. 1-sample tube, 2-level of liquid helium in the sample tube, 3-upper thermometer, 4-quartz beaker, 5-sample, 6-microwave cavity with optical access, 7-quartz windows, 8- ruby crystal, 9-fountain pump, 10-liquid nitrogen shield, 11-level meter, 12-lower thermometer, and 13-lens for collecting light emitted from the sample. (b) Temperature dependence of temperature gradient in vertical direction in the sample tube between two thermometers separated by distance 20.5 cm.

III. INVESTIGATIONS OF THERMOLUMINESCENCE OF NITROGEN NANOCLUSTERS

We studied the thermoluminescence of ensembles of nitrogen nanoclusters containing stabilized nitrogen atoms during warming through the temperature range of 1.25–4.4 K. We warmed up the samples immersed in liquid helium by closing off the pumping of helium vapor from the sample tube containing the liquid helium and waited as the temperature rose from $T \sim 1.25$ to 2.16 K. In this condition, a gradient of temperature existed in the cylindrical volume of helium inside the sample tube. Near T_λ, we pressurized the cryostat

with helium gas to 780 torr and waited as the temperature of the sample increased to 4.4 K. Usually warming up to $T \sim 2.16$ K lasted ~8 min and warming up to $T \sim 4.4$ K lasted ~35 min. Warming up the collection of nanoclusters led to an appearance of intense luminescence. Figure 2(a) shows the dynamics of thermoluminescence of an ensemble of nanoclusters prepared from the gas mixture $[N_2]$:[He] =1:400 in the spectral range of 260–600 nm. The integrated intensity of the spectra obtained during the thermoluminescence process is shown in Fig. 2(b). The α and α' groups of nitrogen atoms, the β and β'' groups of oxygen atoms and Vegard-Kaplan (VK) bands of N_2 molecules are present in the spectra. The α group corresponds to the $^2D \rightarrow {}^4S$ transition of nitrogen atoms, the β group corresponds to the ^{1}S $\rightarrow$ ^{1}D transition of oxygen atoms and the V-K band corresponds to transitions $A^3\Sigma_u^+ \rightarrow X^1\Sigma_g^+$ of N_2 molecules [32]. Figure 2(c) shows the time dependence of α-group and β-group intensities during warming from 1.25 to 4.4 K. There are two intensity maxima of thermoluminescence in this temperature range. The first maximum occurs in superfluid helium at $T \sim 1.9$ K and the second one appears in normal helium at $T \sim 3.25$ K.

In order to understand the nature of the appearance of two maxima in the intensity of thermoluminescence, we studied the behavior of the samples during cycling of warming up and cooling down of the collection of nanoclusters immersed in liquid helium. Figure 3(a) presents the dependence of the thermoluminescence during four consecutive warm ups after subsequent cool down cycles of nanoclusters immersed in superfluid helium from 1.25 to 2.16 K. Figure 3(a) shows that the thermoluminescence intensity for each successive warming process is completely different. The thermoluminescence starts at a higher temperature and monotonically increases with increasing temperature. Also the intensity of thermoluminescence became smaller for each successive warming process. Next, we studied the temperature dependence of thermoluminescence of a collection of nanoclusters during the two consecutive warming up processes over a broader temperature range from 1.25 to 4.4 K and cooling back [see Fig. 3(b)]. In this case, during the first warming of the collection of nanoclusters, the thermoluminescence intensity has two maxima for both nitrogen and oxygen atoms. However, during the second warm up, the thermoluminescence only starts at a higher temperature, $T \sim 4.1$ K, which is close to the final temperature ($T \sim 4.4$) achieved in the first warming, and monotonically increases with temperature [see Fig. 3(b)]. These experiments show that only for as-prepared samples were the intense thermoluminescence observed. The first process of warming changed the sample so that during the following warming processes the luminescence was substantially suppressed. Processes on the surfaces of nanoclusters might be responsible for this behavior.

To study the possible influence of the processes at the surface on the intensity of thermoluminescence, we performed experiments for the samples formed by nanoclusters with different average sizes. Samples formed from nanoclusters with smaller sizes have larger total surface areas. If thermoluminescence is initiated by processes on the surfaces the intensity of luminescence should be larger for these samples. Figure 4 shows the time dependence of thermoluminescence for ensembles of nitrogen nanoclusters with different average

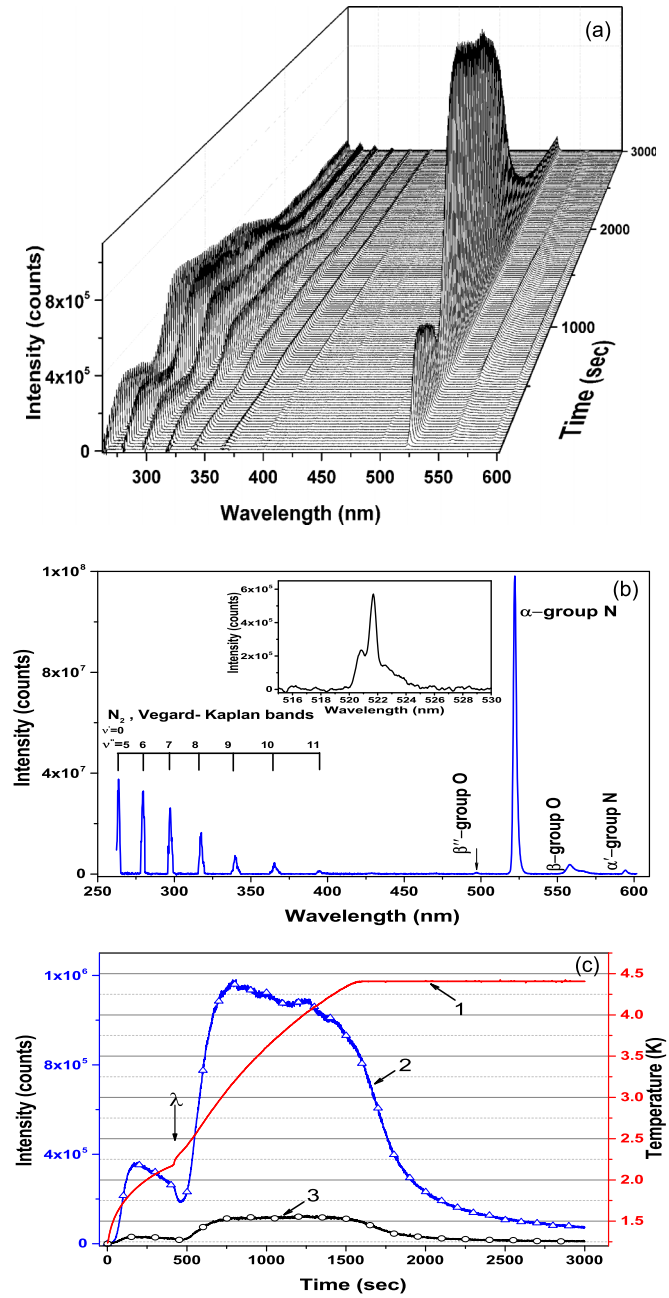

FIG. 2. Thermoluminescence of ensembles of molecular nitrogen nanoclusters with stabilized atoms immersed in liquid helium. (a) Dynamics of thermoluminescence spectra of nitrogen-helium sample during warming up from 1.25 to 4.4 K. Each spectrum in the figure is a sum of 10 spectra taken with exposure time 10 ms. The sample was prepared from a gas mixture [$^{14}N_2$]/[He]=1/400. (b) Integrated thermoluminescence spectra were obtained during the entire warming process. Inset shows the spectrum of the α-group obtained with the spectral resolution 0.05 nm. (c) Time dependence of sample temperature (1). The vertical arrow shows the position of λ point. Time dependence of thermoluminescence intensity for nitrogen (2) and oxygen (3) atoms.

sizes. It is known that reducing the ratio of concentration of the impurity relative to that of helium in the gas jet leads to a decrease in the size of nanoclusters forming porous structures in liquid helium [23]. Reducing the concentration

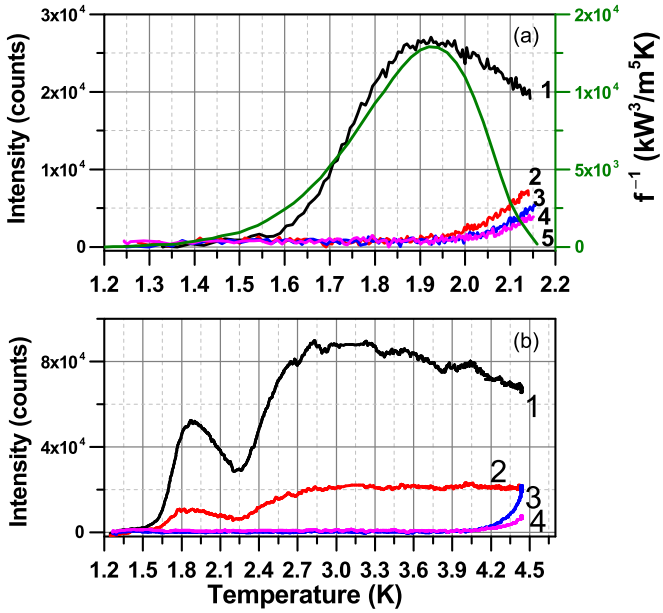

FIG. 3. Temperature dependence of thermoluminescence of nitrogen-helium condensates. (a) Thermoluminescence of nitrogen atoms during warming up from 1.25 to 2.15 K for as prepared sample – 1, during second warming – 2, during third warming – 3, during fourth warming – 4. Heat conductivity function for turbulent HeII – 5 [33]. (b) Thermoluminescence of nitrogen (1) and oxygen (2) atoms during warming up from 1.25 to 4.4 K of as prepared sample and during second warming (3) and (4), correspondingly. Samples were prepared from gas mixture [$^{14}N_2$]/[He]=1/100.

of N_2 molecules from 1% to 0.25% in the nitrogen-helium gas mixture substantially increases the intensity of luminescence of the nanoclusters (see Fig. 4). However, the intensity of luminescence for the sample prepared from an even more dilute gas mixture containing 0.125% of N_2 molecules is smaller than that prepared from gas mixture containing 0.25% of N_2 molecules. This results from the fact that the time for sample

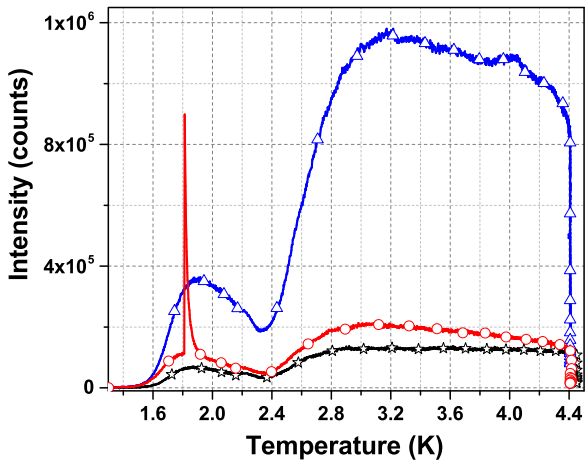

FIG. 4. Temperature dependence of thermoluminescence intensity of nitrogen atoms for samples formed from different gas nitrogen-helium mixtures: 1:100 (black line with open stars), 1:400 (blue line with open triangles), and 1:800 (red line with open circles).

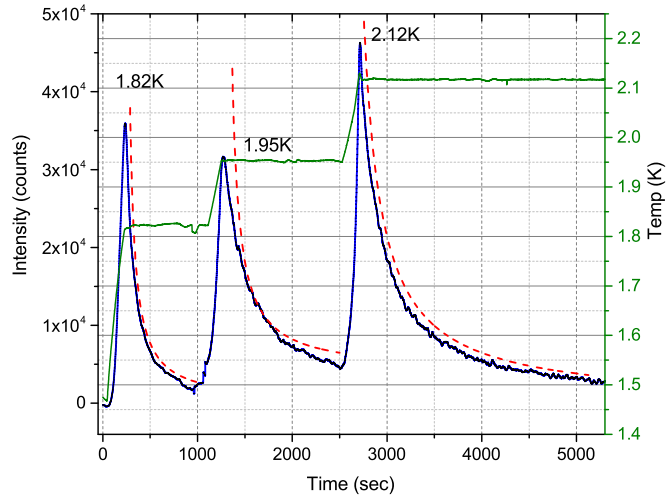

FIG. 5. Kinetics of thermoluminescence intensity for nitrogen nanoclusters (blue line), under step heating from 1.47 to 2.12 K (green line). Red dashed curves were obtained by computer fitting of experimental results in accordance with a hyperbolic law. The sample was prepared from gas mixtures N_2:He=1:400.

preparation was the same but the total quantity of the sample prepared from the more dilute mixture is twice smaller, and therefore the sample only partially fills the observation region. During the investigation of the nanoclusters prepared from the gas mixture containing 0.125% of N_2 molecules we observed a thermal explosion inside HeII. The explosion provided an intense emission, shown as a sharp peak on the red curve of Fig. 4. From these experiments, we can conclude that increasing of the surface area in the ensemble of nanoclusters results in enhancement of intensity of thermoluminescence.

The investigation of thermoluminescence decay at constant temperature could also provide information on the origin of thermoluminescence. The most intense feature of the observed thermoluminescence is the α group of nitrogen atoms. In the solid nitrogen, the α-group decays exponentially with a characteristic time of ~30 s [32]. We studied the decay of the α group of nitrogen atoms in a collection of molecular nitrogen nanoclusters immersed in superfluid helium at constant temperature. In these experiments, the ensemble of nitrogen nanoclusters was prepared from a gas mixture N_2:He=1:400 at $T \sim 1.5$ K. After stopping the discharge, we waited until the afterglow became weak. Stepwise increasing of the temperature led to a strong enhancement of the thermoluminescence. A typical dependence of the thermoluminescence intensity on the temperature of the nanoclusters during the three-stage step heating is presented in Fig. 5. The time dependence of themoluminescence intensity (I) at any constant temperature below T_λ is best described by the hyperbolic law $I \sim t^{-1}$ and the characteristic decay time is substantially longer compared to that in solid nitrogen [32].

IV. ELECTRON SPIN RESONANCE INVESTIGATIONS OF NITROGEN ATOMS STABILIZED IN MOLECULAR NITROGEN NANOCLUSTERS

To understand the role of stabilized nitrogen atoms in the appearance of thermoluminescence, we performed

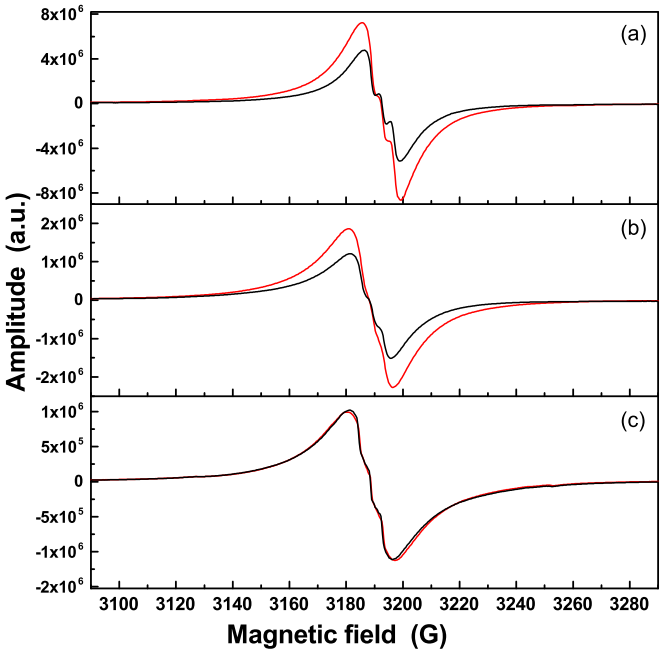

FIG. 6. (a) Comparison of the ESR spectra for as-prepared samples (black) and after warming to 4.4 K (red). Spectra were obtained for samples prepared from nitrogen-helium mixtures $[N_2]$:[He] = 1:100 (a), 1:400 (b), and 1:800 (c).

investigations by the ESR method. Via this technique, measurements of concentrations of nitrogen atoms stabilized in nanoclusters immersed in liquid helium were carried out during the process of warming. The ESR spectra of N(^{4}S) atoms were obtained for all samples described in the previous section. The spectra were recorded at temperature $T \sim 1.32$ K, just before warming the samples, and again after cycles of warming up to temperatures of either 2.16 or 4.4 K followed by cooling back down to $T \sim 1.3$ K. It was found that annealing of the samples to 2.16 K does not change of any of the measured ESR signals. However, as can be seen from Fig. 6, annealing of the samples to 4.4 K resulted in an increase of the ESR signals for two of the samples prepared from gas mixtures $[N_2]$:[He]=1:100 and $[N_2]$:[He]=1:400 but does not change the signal of the sample prepared from the $[N_2]$:[He] = 1:800 gas mixture. Figure 6 shows the comparison of the ESR spectra of N(^{4}S) atoms for as-prepared samples and then after warming to 4.4 K. The increase of the ESR signals of N atoms during warming in HeI for two samples indicates that after preparation, the samples had a larger volume than could be placed in the ESR cavity. During warming up above T_λ some material, which was initially accumulated in the beaker above the ESR cavity, entered into the sensitive zone of the ESR cavity. In the case of the sample prepared from the $[N_2]$:[He] = 1:800 gas mixture the initial volume of the sample was small so the entire sample was in the sensitive zone of the ESR cavity from the beginning. The average concentrations of N(^{4}S) were calculated by comparison between double integrals of ESR signals of the N(^{4}S) atoms and those from ruby signals under the same experimental conditions. Table I shows the average concentrations of N atoms stabilized in the samples prepared from different nitrogen-helium gas mixtures. As

TABLE I. Average concentration of N atoms in the samples prepared from different nitrogen-helium gas mixtures.

Gas mixtures $[^{14}N_2]$/[He]	Average concentration, cm^{-3}
1/100	5.09×10^{18}
1/400	2.47×10^{18}
1/800	1.21×10^{18}

can be seen from the Table 1, all of the samples studied contained high average concentrations of stabilized nitrogen atoms. The average concentrations of N atoms were in the range between 1.2×10^{18} and 5×10^{18} cm^{-3}. The dipolar magnetic interaction between electron spins is the dominant line broading mechanism in this system. This allows local concentrations of nitrogen atoms to be estimated by the following formula [34]:

$$\Delta H_{pp} = 2.3 g \mu_0 \sqrt{S(S+1)} n_l, \quad (1)$$

modified for N atoms ($n_l = 5.4 \times 10^{18}\, \Delta H_{pp}$), where ΔH_{pp} is the peak to peak width of the ESR lines in Gauss, and n_l is the local concentration of the atoms in cm^{-3}. The characteristic features of the ESR spectra of N atoms in as-prepared samples are the broad wings and weak triplet at the central part (see Fig. 6). All features of experimental ESR lines can be fitted with a sum of three triplets of Lorentzian lines, as shown in Fig. 7. The fitting process was performed by a Graphic User Interface (GUI) program written in MATLAB. This GUI program can simulate the experimental signal using up to eight Lorentzian/Gaussian function components. It automatically searches for the best hyperfine splitting constant and linewidth corresponding to each triplet. When the difference between

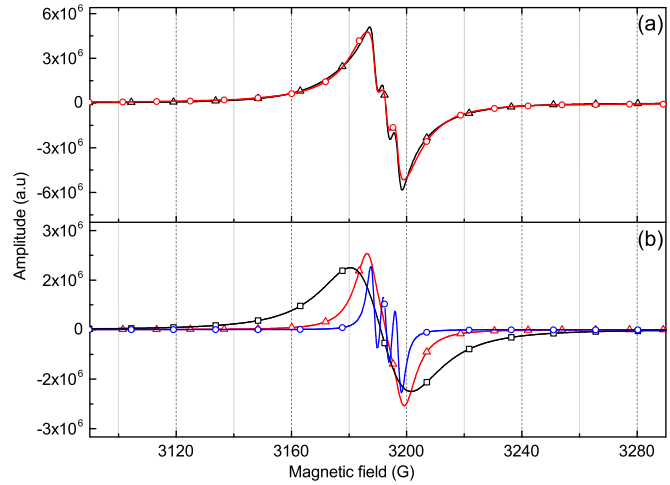

FIG. 7. Experimental ESR spectrum of N atoms for an as-prepared nitrogen-helium sample formed by the $[^{14}N_2]$/[He]=1/100 gas mixture is shown as a black line with open triangles (a). The sum of the fitting lines is shown as red line with circles (a). Three triplets of fitting lines used for decomposing the experimental ESR spectrum are shown in (b): blue line with circles is a triplet of Lorentzian lines with the width 3.2 G, red line with open triangles is a triplet of Lorentzian lines with the width 8.7 G, and black line with squares is a triplet of Lorentzian lines with the width 19.1 G.

TABLE II. Hyperfine constants A, g factor, peak to peak line widths, ΔH_{pp}, and local concentrations of N atoms in nitrogen-helium condensates obtained from ESR line fittings. [Illustrated in Fig. 7(b) for the 1:100 sample].

Gas mixtures, N_2:He	Curve type	A (G)	g factor	ΔH_{pp} (G)	Local concentration, n_N cm^{-3}	Weight (%)
1:100	Lorentzian	4.00	2.0020	19.1	1.03×10^{20}	77.9
	Lorentzian	4.20	2.0020	8.7	4.69×10^{19}	18.4
	Lorentzian	4.10	2.0020	3.2	1.73×10^{19}	3.7
1:400	Lorentzian	4.00	2.0022	24.7	1.33×10^{20}	80.2
	Lorentzian	4.20	2.0022	10.1	5.45×10^{19}	19.8
1:800	Lorentzian	4.00	2.0021	35.2	1.90×10^{20}	67.2
	Lorentzian	4.20	2.0021	12.5	6.75×10^{19}	32.8

the simulated and experimental curves becomes minimal, the program stops searching and gives the corresponding parameters. Figure 7(a) shows an experimental ESR spectrum for N atoms in the collection of nanoclusters prepared from the [$^{14}N_2$]/[He]=1/100 gas mixture, and the sum of the three fitting triplets, which provide rather good agreement with the experimental spectra. Figure 7(b) shows three fitting lines composed of the triplets with different hyperfine splittings and linewidths. Each of the triplets could be assigned to atoms in specific environments. A similar analysis was performed on all spectra obtained for samples prepared from different nitrogen-helium gas mixtures. Some spectra could be fitted with a sum of two triplets of Lorentzian lines. The local concentration was estimated for each of the respective fitting lines by using Eq. (1). The results of this analysis are presented in Table II.

In a previous study, it has been found that fitting lines with larger widths belong to N atoms located on the surface of the N_2 nanoclusters, and the fitting lines with smaller widths can be assigned to N atoms stabilized inside the N_2 nanoclusters [29]. The spectroscopic characteristics (A values and g factors) obtained support this conclusion. The local concentrations of atoms, $(1-2) \times 10^{20}$ cm^{-3}, determined from the width of ESR spectra were considerably larger than the average concentrations. The much larger local concentration is an expected consequence of the high porosity of the sample. From the results obtained, we can also conclude that decreasing the size of the nanoclusters by reducing the content of N_2 molecules in a condensed nitrogen-helium gas mixture leads to increasing the local concentration of N atoms residing on the surfaces of the N_2 nanoclusters. Analysis of the ESR spectra of nitrogen atoms stabilized in the nanoclusters also provided evidence that most of the atoms (70%–80%) resided on the surfaces of the nanoclusters. The collection of nanoclusters with high concentrations of N atoms on their surfaces is very promising for observing chemical reactions if the collisions of the nanoclusters could be initiated. However, the ESR measurements show that high concentrations of N atoms are not reduced during the process of warming samples in liquid helium and do not show any sign of nitrogen atom recombination. Possibly only a small portion of the atoms can participate in the process of recombination but their quantity could not be determined by the ESR method because the majority of atoms are stable and continue to produce a large ESR signal.

V. DETERMINATION OF THE NUMBER OF PHOTONS EMITTED DURING WARMING OF A SAMPLE IMMERSED IN LIQUID HELIUM

We performed experiments to determine the absolute number of photons emitted from the collection of nanoclusters during the process of thermoluminescence. This number provides an estimate of the number of N atoms participating in the process of thermoluminescense. The details of these measurements can be found elsewhere [35]. The measurements were performed with a collection of nanoclusters prepared from the [N_2]:[He] = 1:400 gas mixture. First, we recorded the intensity of thermoluminescence during the entire process of warming from 1.25 to 4.4 K. A Hamamatsu photomultiplier tube (PMT) R928 was used to detect the emitted light. The output of the PMT was fed into a LeCroy oscilloscope. The dependence of intensity of the thermoluminescence on time was similar to that shown in Fig. 2(c). The integrated signal on oscilloscope was calculated as $I = 2411$ V s over the entire warming of the sample. From the geometry of the experiment, the solid angle for detecting light from the sample was estimated as $d\Omega = 0.033$ radians. Second, we performed calibration of the PMT by using an Ocean Optics DH-2000 balanced halogen source with known output power. It was found that the 1V amplitude of the signal on the oscilloscope corresponding to the power of light detected by the PMT (P) was equal to $P = 4.27 \times 10^{-5}$ μW. Taking into consideration this information, we can calculate the total energy of the light emitted by the sample during the entire warming period, $E_{\rm tot} = P \times I \times 4\pi/d\Omega = 3.92 \times 10^{-5}$ J. The most intense emission in the thermoluminescence corresponds to the α-group of nitrogen atoms at $\lambda \sim 523$ nm. The energy of a photon which corresponds to this wavelength is $E_{\rm ph} = 3.8 \times 10^{-19}$ J. The total number of photons emitted from the sample during warming from 1.25 to 4.4 K is equal to $E_{\rm tot}/E_{\rm ph} = \sim 1 \times 10^{14}$. This fact means that only a small fraction ($\sim 4 \times 10^{-5}$) of all atoms contributed to the thermoluminescence processes. The integrated intensity of thermoluminescence in HeII is approximately one order magnitude less than that in HeI, leading us to the estimate that an even smaller fraction of nitrogen atoms ($\sim 4 \times 10^{-6}$) was emitted during the process of warming up in HeII. If we assume that the emission of N atoms is a consequence of nitrogen atom recombination, we can conclude that $\sim 1 \times 10^{14}$ atoms should recombine in HeII during the process of thermoluminescence. The change in the

number N atoms at this level can thus not be determined by the ESR method in the presence of the very large concentration ($\sim 2.5 \times 10^{18}$ cm^{-3}) of stabilized nitrogen atoms.

VI. DISCUSSION

We have studied the temperature dependence of the thermoluminescence of molecular nitrogen nanoclusters containing high concentrations of stabilized atoms immersed in liquid helium. Two thermoluminescence maxima were observed, one in superfluid helium at $T \sim 1.9$ K and another at $T \sim 3.2$ K. It is natural to assign the appearance of thermoluminescence to the recombination of nitrogen atoms stabilized on the surfaces of nanoclusters immersed in liquid helium. Only the mechanisms initiating nitrogen atom recombination at low temperatures should then be considered.

Thermoluminescence of samples in HeI can be explained by thermal explosions of a small fraction of the nanoclusters initiated by the process of association of nanoclusters. It has been observed in x-ray experiments on collections of nanoclusters immersed in liquid helium that the nanoclusters grow during warming in HeI [22,28,36]. Thus the density of the porous structure formed by collections of nanoclusters increases. The increase of the ESR signals of N atoms during warming in HeI obtained in this work also indicates that the increase of the density of the sample is due to the entrance of additional nanoclusters which were initially accumulated in the beaker above the sensitive zone of the ESR cavity. The growth in size of the nanoclusters was also accompanied by collapsing of the pores in the samples in HeI. As the nanoclusters made contact, pairs of N atoms on the surfaces could recombine, eventually leading to energy release inside nanoclusters and initiation of recombination of other N atoms contained in these nanoclusters. From the comparison of the N atom concentration measured by ESR and estimates of the number of emitting atoms during thermoluminescence, we can conclude that only a negligible fraction of all the atoms ($\sim 4 \times 10^{-5}$) participate in emission. The poor thermal conductivity of liquid helium at temperatures above T_λ does not allow the heat, released as a result of chemical reactions, to spread rapidly to other nanoclusters. This tends to isolate explosions to small regions of the sample.

The observation of thermoluminescence in HeII is a more unusual phenomenon even if we consider that the collection of molecular nitrogen nanoclusters contain a high density of stored energy. Thermoluminescence in HeII is approximately one order of magnitude less intense than in HeI. It is difficult to satisfy the conditions for initiation of thermal explosions of nanoclusters in HeII because of the effective heat removal from nanoclusters by the superfluid helium [35]. Even if recombination of N atoms occurs in nanoclusters immersed in HeII, the N_2 molecules are formed at high vibrational states. The vibrational relaxation of N_2 molecules is rather slow (~ 1 s) [37–39] and the energy released can be easily removed by the superfluid helium [33] thus preventing chain reactions of stabilized atoms in nanoclusters, and thermal explosions of nanoclusters. We did not observe any structural changes of the collection of nanoclusters immersed in HeII and the ESR signal was unchanged during the warming process in HeII. The fraction of nitrogen atoms participating in thermoluminescence in HeII was rather small, of order ($\sim 4 \times 10^{-6}$).

The thermoluminescence of nitrogen atoms in samples formed by injecting products of a gas discharge into superfluid helium was studied earlier [40,41]. The thermoluminescence initially was assigned to the emission of N(^{2}D)-N_2 van der Waals complexes in solid helium. It was suggested that solid helium could be formed by injection of single heavy atoms and molecules into superfluid helium [42]. Via this model, single metastable N(^{2}D) atoms and N_2 molecules could be captured in solid helium. The thermally activated diffusion of these species in solid helium would then lead to the formation of N(^{2}D)-N_2 van der Waals complexes where the probability of optical transition N(^{2}D $\leftarrow$ ^{4}S) of metastable nitrogen atom is substantially enhanced [40]. However, structural studies of the samples formed in HeII did not find the presence of single atoms or molecules in solid helium but instead provided strong evidence that the sample consisted of a porous collection of molecular nitrogen nanoclusters with the pores filled with superfluid helium [22,23]. Complementary ESR studies showed that all of the stabilized atoms reside in the nanoclusters [26,43]. Recently, another mechanism of N atom themoluminescence in HeII was discussed [41]. The authors of Ref.[41] suggested that electrons and nitrogen ions would be captured separately in molecular nitrogen nanoclusters during the process of injection of discharge products in HeII at $T = 1.5$ K. They proposed that increasing the temperature of the ensembles of nanoclusters immersed in HeII could initiate the release of electrons from the traps. After that, the electrons could tunnel through the nanoclusters resulting in electron-ion recombination [41]. The nitrogen molecules so excited could emit light or transfer energy to stabilized nitrogen atoms thereby initiating α-group emission. In contrast, in our experiments, we did not observe any ESR signal from electrons or ions in the samples immersed in HeII. Electrons and nitrogen anions were only detected during the process of destruction of the sample, where these species could be formed during the fast release of stored energy [44,45]. Additionally, none of the above mechanisms could explain the temperature dependence of the thermoluminescence observed in this work.

We explain the thermoluminescence of collections of nanoclusters immersed in HeII as a result of recombination of nitrogen atoms stabilized on the surface of nanoclusters. We suggest that the process of atom recombination might be initiated by quantum vortices created when the heat flux is applied. The rationale is as follows. The resulting vortex density L is given by

$$L^{1/2} = \gamma(T)\, u_{\rm ns}, \tag{2}$$

where $u_{\rm ns}$ is the relative velocity of the normal and superfluid components, and the coefficient $\gamma(T)$ has been measured experimentally [6]. For counterflow, $u_{\rm ns}$ is related to the applied heat flux according to

$$u_{\rm ns} = \frac{q}{\rho_s s T}, \tag{3}$$

where ρ_s is the superfluid density and s is the specific entropy of HeII. The resulting flux density is given by

$$L^{1/2} = \gamma(T)\, \frac{q}{\rho_s s T}. \tag{4}$$

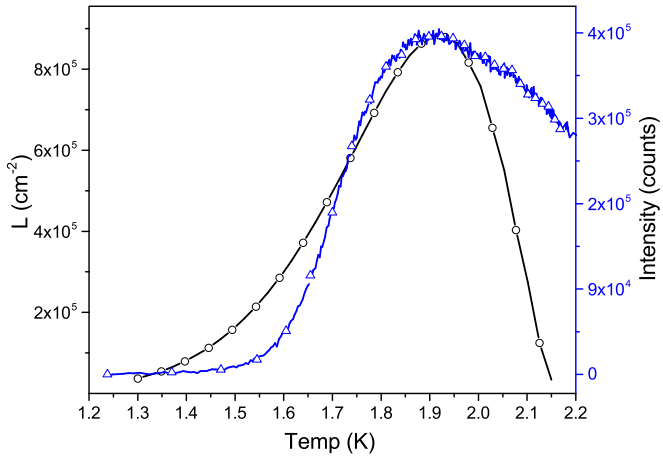

FIG. 8. Dependence of vortex density on temperature in superfluid helium during observation of thermoluminescence from the ensemble of nitrogen nanoclusters (circles) and temperature dependence of thermoluminescence intensity of nitrogen atoms for the sample formed from $[N_2]$:[He] = 1:400 gas mixture (triangles).

For the case of an applied temperature gradient dT/dx, the heat flux is described by the Gorter-Mellink heat transport formula

$$q = -\left[f^{-1}(T,P)\frac{dT}{dx}\right]^{1/3}, \tag{5}$$

where

$$f^{-1}(T,P) = f^{-1}(T_\lambda,P)\left\{\left(\frac{T}{T_\lambda}\right)^{5.7}\left[1-\left(\frac{T}{T_\lambda}\right)^{5.7}\right]\right\}^3 \tag{6}$$

is the heat conductivity function for turbulent flow [33,46]. If we consider also the dependence on temperature of the superfluid density of helium

$$\rho_s = \rho\left(\frac{T}{T_\lambda}\right)^{5.6} \tag{7}$$

and entropy

$$s = 1.5838\left(\frac{T}{T_\lambda}\right)^{5.6}, \tag{8}$$

we can construct a graph of the dependence of the vortex density on temperature for the experimentally measured temperature gradient in superfluid helium shown in Fig. 1(b). Figure 8 shows the dependence on temperature of the vortex density in the case of an existing gradient of temperature in the bulk helium. This dependence has a maximum at a temperature ~1.9 K. The shape of this dependence is determined by the heat conductivity function for turbulent HeII, $f^{-1}(T,P)$, which is shown as curve 5 in Fig. 3(a) [33]. In Fig. 8, we also show the temperature dependence of the thermoluminescence of ensembles of nanoclusters during warming in HeII. The temperature dependence of the thermoluminescence intensity for as-prepared ensembles of nanoclusters is in reasonable agreement with the temperature dependence of the vortex density for the conditions of our experiments. It is significant that the maximum thermoluminescence intensity occurs at the same temperature as the maximum vortex density in bulk HeII. The estimate of the heat flux during the process of warming our samples is 25–30 mW cm^{-2}. This value is larger than the critical value for the creation of turbulence in bulk HeII [47]. These facts provide some evidence of the involvement of vortices created in superfluid helium for the initiation of the thermoluminescence of nitrogen atoms at such low temperatures. The mechanism of initiation of thermoluminescence by vortices may involve the following steps. When a heat flux is applied to the sample immersed in HeII, vortices are created in the bulk helium and in the pores of the sample. Superfluid helium easily penetrates through the interconnected pores of the sample. The temperature gradient in the samples should be larger than in bulk helium, so the efficiency of creation of vortices in the pores should be more efficient than in the bulk helium. Samples contain strands of nanoclusters. Some strands can be attached only by one end to the main porous structure. Vortices can attract and capture in the vortex cores the free swimming strands of the nanoclusters. In the vortex cores, the collisions of nanoclusters from different strands take place. The collisions of nanoclusters in the vortex cores can initiate recombination of N atoms that reside on the surface of the nanoclusters. As a result of this recombination the neighboring strands become connected together by newly formed chemical bonds. The excited molecules formed as a result of recombination of nitrogen atoms can emit light (V-K bands) or transfer energy to nitrogen and oxygen atoms stabilized in nanoclusters which then emit α -group and β-group spectra, respectively. The temperature dependence of the intensity of emission for all species is correlated with the temperature dependence of the vortex density in HeII. The suppression of thermoluminescence during the *later* processes of warming and cooling down demonstrated in Fig. 3 can be explained by a reduction in the number of free strands available needed for nitrogen atom recombination. This may be a consequence of the formation of chemical bonds between adjacent strands of nanoclusters during the first warm-up.

The suggestion that we observed quantum vortex induced thermoluminescence was also supported by experiments with ensembles of nanoclusters with different sizes. When the sizes of nanoclusters are reduced, the frequency of their collisions in the vortex core increases and the overall available surface for possible interactions in the case of smaller clusters increases. Additionally, for the smaller size clusters the probability for reaction of two nitrogen atoms residing on the surfaces of different nanoclusters per collision should increase. In fact, we observed experimentally (see Table II) that nanoclusters with smaller sizes were characterized by larger local concentration of nitrogen atoms stabilized at the surfaces of the nanoclusters. All these factors lead to the increasing intensity of thermoluminescense for the ensembles of nanoclusters of smaller sizes. In the sample with the smallest size of nanoclusters prepared from a gas mixture containing 0.125% of N_2 molecules, vortex-induced recombination of stabilized atoms results in the initiation of a chain reaction of nitrogen atoms in some nanoclusters and their thermal explosion. As evidence of this process, a sharp thermoluminescence peak was observed at $T \sim 1.9$ K, where the efficiency of vortex formation in HeII in our experimental conditions reaches a maximum (see Fig. 4). The local concentration of N atoms stabilized on the surface of nanoclusters in this sample was maximal in our experiments

and was equal to 2×10^{20} cm^{-3}. However, only a small fraction of the nanoclusters immersed in HeII was destroyed in this explosion as indicated by the small number of photons ($\sim 10^{12}$) detected during the explosion.

Further evidence that thermoluminescence is connected with the vortices in HeII was obtained from the decay of thermoluminescence at constant temperatures $T = 1.82, 1.95$, and 2.12 K following step heating. A similar result for α-group decay was previously observed [40]. In solid nitrogen, the characteristic decay time of the α group is 30 s and the thermoluminescence intensity of nitrogen atoms should be negligible after 200 seconds following termination of excitation. The observed long decay of the thermoluminescence of collections of nanoclusters provides evidence that an additional mechanism for excitation of nitrogen atoms exists in superfluid helium. This source of excitation is quantum vortices, which continued to initiate recombination of nitrogen atoms and their luminescence even when the temperature of the sample was kept constant. Thus the thermoluminescence decay is consistent with a hyperbolic law decay of the vortex densities in superfluid helium [1,48]. A long time decay of the vortex density with a similar characteristic time (hours) was observed in Ref. [48]. We suggested that the long decay of the vortices occurred in the voids of the sample, and in the bulk helium surrounding the sample. From the decay time of the luminescence observed, the size of the voids in the sample was estimated to be $\sim$0.3 cm. Recently, it was recognized that only for small heat fluxes (less than 50 mw/cm^2) does the vortex density decay approximately according to a hyperbolic law [49]. The estimate of the heat flux during the process of warming our samples is 25–30 mW cm^{-2}, which is in the range where the hyperbolic decay of the vortices should be observed.

VII. CONCLUSIONS

In summary, we developed a new experimental approach for studying chemical reactions in porous structures formed by nanoclusters containing stabilized atoms immersed in liquid helium. We have observed chemical reactions in porous ensembles of nanoclusters immersed in superfluid helium, which might be induced by quantum vortices. These observations might open new possibilities for studying chemical reactions of heavy species initiated by vortices at very low temperatures in HeII where diffusion and tunneling in solid nanocrystallites are completely suppressed. We also observed the thermoluminescence of ensembles of nitrogen nanoclusters in normal liquid helium which was initiated by association of the nanoclusters resulting in thermal explosions of a small fraction of the nanoclusters containing high concentrations of stabilized nitrogen atoms. Thermal explosions occur due to chain reactions of nitrogen atoms in nanoclusters under the conditions of poor thermal heat removal by the surrounding liquid helium.

ACKNOWLEDGMENTS

This work was supported by NSF Grant No. DMR 1209255, Welch Foundation Grant No. A 1884, and AFOSR Grant No. FA9550-18-1-0100.

[1] W. F. Vinen, An introduction to quantum turbulence, J. Low Temp. Phys. **145**, 7 (2006).
[2] C. F. Barenghi, L. Skrbek, and K. R. Sreenivasan, Introduction to quantum turbulence, Proc. Natl. Acad. Sci. USA **111**, 4647 (2014).
[3] Y. A. Sergeev and C. F. Barenghi, Particles-vortex interactions and flow visualization in ^{4}He, J. Low Temp. Phys. **157**, 429 (2009).
[4] G. P. Bewley, D. P. Lathrop, and K. R. Sreenivasan, Visualization of quantized vortices, Nature (London) **441**, 588 (2006).
[5] W. Guo, J. D. Wright, S. B. Cahn, J. A. Nikkel, and D. N. McKinsey, Metastable Helium Molecules as Tracers in Superfluid ^{4}He, Phys. Rev. Lett. **102**, 235301 (2009).
[6] S. Babuin, M.Stammeier, E. Varga, M. Rotter, and L. Skrbek, Quantum turbulence of bellow-driven ^{4}He superflow: Steady state, Phys. Rev. B **86**, 134515 (2012).
[7] D. E. Zmeev, F. Pakpour, P. M. Walmsley, A. I. Golov, W. Guo, D. N. McKinsey, G. G. Ihas, P. V. E. McClintock, S. N. Fisher, and W. F. Vinen, Excimers He_2^* as Tracers of Quantum Turbulence in ^{4}He in the T=0 Limit, Phys. Rev. Lett. **110**, 175303 (2013).
[8] W. Guo, M. LaMantia, D. P. Lathrop, and S. W. Van Sciver, Visualization of two-fluid flows of superfluid helium-4, Proc. Natl. Acad. Sci. USA **111**, 4653 (2014).
[9] G. P. Bewley, M. S. Paoletti, K. R. Sreenivasan, and D. P. Lathrop, Characterization of reconnecting vortices in superfluid helium, Proc. Natl. Acad. Sci. USA **105**, 13707 (2008).
[10] E. Fonda, D. P. Meichle, N. T. Ouellette, S. Hormoz, and D. P. Lathrop, Direct observation of Kelvin waves excited by quantized vortex reconnection, Proc. Natl. Acad. Sci. USA **111**, 4707 (2014).
[11] P. M. Walmsley, A. I. Golov, H. E. Hall, A. A. Levchenko, and W. F. Vinen, Dissipation of Quantum Turbulence in the Zero Temperature Limit, Phys. Rev. Lett. **99**, 265302 (2007).
[12] P. Walmsley, D. Zmeev, F. Pakpour, and A. Golov, Dynamics of quantum turbulence of different spectra, Proc. Natl. Acad. Sci. USA **111**, 4691 (2014).
[13] E. B. Gordon, A. V. Karabulin, V. I. Matyushenko, V. D. Sizov, and I. I. Khodos, Structure of metallic nanowires and nanoclusters formed in superfluid helium, J. Exp. Theor. Phys. **112**, 1061 (2011).
[14] E. B. Gordon, A. V. Karabulin, V. I.Matyushenko, V. D. Sizov, and I. I. Khodos, The role of vortices in the process of impurity nanoparticles coalescence, Chem. Phys. Lett. **519–520**, 64 (2012).
[15] L. F. Gomez, E. Loginov, and A. F. Vilesov, Traces of Vortices in Superfluid Helium Droplets. Phys. Rev. Lett. **108**, 155302 (2012).
[16] L. F. Gomez *et al.*, Shapes and vorticies of superfluid helium nanodroplets, Science **345**, 906 (2014).
[17] M. C. Tsatsos, P. E. S. Tavares, A. Cidrim, A. R. Fritsch, M. A. Caracanhas, F. E. A. dos Santos, C. F. Barenghi, and V. S. Bagnato, Quantum turbulence in trapped atomic Bose-Einstein condensates, Phys. Rep. **622**, 1 (2016).

[18] M. H. W. Chan, K. I. Blum, S. Q. Murphy, G. K. S. Wong, and J. D. Reppy, Disorder and the Superfluid Transition in Liquid ^{4}He, Phys. Rev. Lett. **61**, 1950 (1988).

[19] J. D. Reppy, Superfluid Helium in porous media, J. Low Temp. Phys. **87**, 205 (1992).

[20] J. Yoon, D. Sergatskov, J. Ma, N. Mulders, and M. H. W. Chan, Superfluid Transition of ^{4}He in Ultralight Aerogel, Phys. Rev. Lett. **80**, 1461 (1998).

[21] R. Toda, M. Hieda, T. Matsushita, N. Wada, J. Taniguchi, H. Ikegami, S. Inagaki, and Y. Fukushima, Superfluidity of ^{4}He in One and Three Dimensions Realized in Nanopores, Phys. Rev. Lett. **99**, 255301 (2007).

[22] V. Kiryukhin, B. Keimer, R. E. Boltnev, V. V. Khmelenko, and E. B. Gordon, Inert-gas Solids with Nanoscale Porosity, Phys. Rev. Lett. **79**, 1774 (1997).

[23] V. Kiryukhin, E. P. Bernard, V. V. Khmelenko, R. E. Boltnev, N. V. Krainyukova, and D. M. Lee, Noble-gas Nanoclusters with Fivefold Symmetry Stabilized in Superfluid Helium, Phys. Rev. Lett. **98**, 195506 (2007).

[24] S. I. Kiselev, V. V. Khmelenko, D. M. Lee, V. Kiryukhin, R. E. Boltnev, E. B. Gordon, and B. Keimer, Structural studies of impurity-helium solids, Phys. Rev. B **65**, 024517 (2001).

[25] S. Mao, R. E. Boltnev, V. V. Khmelenko, and D. M. Lee, ESR studies of nitrogen atoms stablized in aggregates of krypton-nitrogen nanoclusters immersed in superfluid helium, Low Temp. Phys. **38**, 1037 (2012).

[26] E. P. Bernard, R. E. Boltnev, V. V. Khmelenko, and D. M. Lee, Stabilization of high concentrations of nitrogen atoms in impurity-helium solids, J. Low Temp. Phys. **134**, 199 (2004).

[27] E. B. Gordon, L. P. Mezhov-Deglin, and O. F. Pugachev, Stabilization of nitrogen atoms in superfluid helium, J. Exp. Theor. Phys. Lett. **19**, 103 (1974).

[28] V. V. Khmelenko, H. Kunttu, and D. M. Lee, Recent progress in studies of nanostructured impurity-helium solids, J. Low Temp. Phys. **148**, 1 (2007).

[29] S. Mao, A. Meraki, P. T. McColgan, V. Shemelin, V. V. Khmelenko, and D. M. Lee, Experimental setup for investigation of nanoclusters at cryogenic temperatures by electron spin resonance and optical spectroscopies, Rev. Sci. Instrum. **85**, 073906 (2014).

[30] P. T. McColgan, A. Meraki, R. E. Boltnev, D. M. Lee, and V. V. Khmelenko, Optical and electron spin resonance studies of destruction of porous structures formed by nitrogen-rare gas nanoclusters in bulk superfluid helium, J. Low Temp. Phys. (2016), doi:10.1007/s10909-016-1707-5.

[31] V. Arp, Heat transport through helium II, Cryogenics **10**, 96 (1970).

[32] O. Oehler, D. A. Smith, and K. Dressler, Luminescence spectra of solid nitrogen excited by electron impact, J. Chem. Phys. **66**, 2097 (1977).

[33] S. W. Van Sciver, *Helium Cryogenics*, 1st ed. (Plenum, New York and London, 1986), p. 144.

[34] C. Kittel and E. Abrahams, Dipolar broadening of magnetic resonance lines in magnetically diluted crystals, Phys. Rev. **90**, 238 (1953).

[35] See Supplemental Material at http://link.aps.org/supplemental/10.1103/PhysRevB.95.104502 for additional optical investigation.

[36] S. I. Kiselev, V. V. Khmelenko, D. M. Lee, V. Kiryukhin, R. E. Boltnev, E. B. Gordon, and B. Keimer, X-ray studies of structural changes of impurity-helium solids, J. Low Temp. Phys. **126**, 235 (2002).

[37] A. A. Ovchinnikov, Localized long-lived vibrational states in molecular crystals, Sov. Phys. J. Exp. Theor. Phys. Lett. **30**, 147 (1970).

[38] K. Dressler, O. Oehler, and D. A. Smith, Measurement of Slow Vibrational Relaxation and Fast Vibrational Energy Transfer in Solid N_2, Phys. Rev. Lett. **34**, 1364 (1975).

[39] K. Takizawa, A. Takami, and S. Koda, Decay kinetics of N(^2P or ^2D) + $N_2(X^1\Sigma_g^+, \nu'')$ in low temperature solid nitrogen, J. Phys. Chem. A **104**, 3693 (2000).

[40] R. E. Boltnev, E. B. Gordon, V. V. Khmelenko, I. N. Krushinskaya, M. V. Martynenko, A. A. Pelmenev, E. A. Popov, and A. F. Shestakov, Luminescence of nitrogen and neon atoms isolated in solid helium, Chem. Phys. **189**, 367 (1994).

[41] A. A. Pelmenev, I. N. Krushinskaya, I. B. Bykhalo, and R. E. Boltnev, On charged impurity structures in liquid helium, Low Temp. Phys. **42**, 224 (2016).

[42] E. B. Gordon, V. V. Khmelenko, A. A. Pelmenev, E. A. Popov,, and O. F. Pugachev, Impurity-helium van der Waals crystals, Chem. Phys. Lett. **155**, 301 (1989).

[43] R. E. Boltnev, I. N. Krushinskaya, A. A. Pelmenev, E. A. Popov, D.Yu. Stolyarov, and V. V. Khmelenko, Study of stabilization and recombination of nitrogen atoms in impurity-helium condensates, Low Temp. Phys. **31**, 547 (2005).

[44] I. N. Krushinskaya, R. E. Boltnev, I. B. Bykhalo, A. A. Pelmenev, V. V. Khmelenko, and D. M. Lee, Optical spectroscopy and current detection during warm-up destruction of impurity-helium condensates, Low Temp. Phys. **41**, 541 (2015).

[45] R. E. Boltnev, I. B. Bykhalo, I. N. Krushinskaya, A. A. Pelmenev, S. Mao, A. Meraki, P. T. McColgan, D. M. Lee, and V. V. Khmelenko, Spectroscopic observation of nitrogen anions N^- in solid matrices, Phys. Chem. Chem. Phys. **18**, 16013 (2016).

[46] S. W. Van Sciver, Heat transfer through an extended surface containing He II, Trans. ASME: J. Heat Transfer **121**, 142 (1999).

[47] W. F. Vinen, Mutual friction in a heat current in liquid Helium-II. 1. Experiment on steady heat current, Proc. R. Soc. London A **249**, 114 (1957).

[48] D. D. Awschalom and K. W. Schwarz, Observation of a Remanent Vortex-Line Density in Superfluid Helium, Phys. Rev. Lett. **52**, 49 (1984).

[49] J. Gao, W. Guo, V. S. L'vov, A. Pomyalov, L. Skrbek, E. Varga, and W. F. Vinen, Decay of counterflow turbulence in superfluid ^{4}He, JETP Lett. **103**, 648 (2016).